

## Evaluating MOFs for hydrogen storage under cryogenic conditions

Júlia G. Costa<sup>a</sup>, Débora M. Costa<sup>a</sup>, Andréa S. Pereira<sup>a</sup>, Daniel V. Gonçalves<sup>a</sup>, Sebastião M. P. Lucena<sup>a</sup>

<sup>a</sup>Laboratory of Modeling and 3D Visualization, Department of Chemical Engineering, Universidade Federal do Ceará, Campus do Pici, bl. 709, 60455-760, Fortaleza, CE, Brazil

### Abstract

Hydrogen is an increasingly attractive option for energy storage due to its abundance, non-toxicity, and zero carbon dioxide emissions upon combustion. In this study, we combined molecular simulations and advanced machine learning models to evaluate H<sub>2</sub> cryo-adsorption in metal-organic frameworks (MOFs). The molecular models and forcefields were validated against experimental data from the literature. Grand Canonical Monte Carlo (GCMC) simulations were used to calculate adsorption uptakes in 100 MOFs. Among these, five structures exhibited volumetric capacities greater than 90% of the density of liquid hydrogen. Our findings show that MOFs with low density and high void fraction demonstrated the best performances for cryogenic applications. Additionally, machine learning algorithms were developed to predict H<sub>2</sub> adsorption based on MOF structural characteristics, with XGBoost model delivering the most accurate results. The models developed in this work offer a powerful tool for accelerating the discovery of optimal MOFs for H<sub>2</sub> storage under cryogenic conditions.

**Keywords:** Hydrogen; Metal-organic framework; Cryogenic; Storage;

### 1. Introduction

Hydrogen is one of the most promising candidates for replacing current carbon-based energy sources [1]. H<sub>2</sub> delivery and storage are considered to be a key enabling technology. Liquid hydrogen (LH<sub>2</sub>) is the preferred method for transporting hydrogen due its high volumetric energy density, which significantly reduces costs in transportation and refueling operations. However, due its low boiling point (20 K), the liquefaction of H<sub>2</sub> involves high costs and losses owing its evaporation (boil-off losses), complicating long-term storage and delivery.

Hydrogen storage by cryo-adsorption at 20 K using metal-organic frameworks (MOFs) has been proposed as an alternative to reduce boil-off losses and enhance dormancy during long storage and transportation [2,3]. It was found that the stronger van der Waals interactions between the adsorbate and adsorbent lead to super-dense H<sub>2</sub> adsorption, which compensates for the space occupied by the adsorbent skeleton and results in a volumetric storage capacity comparable to that of LH<sub>2</sub> tanks. Nevertheless, the liquefaction of H<sub>2</sub> remains challenging [4].

A refueling pressure of 100 bar is often used to determine the usable capacity of storage vessels [5]. H<sub>2</sub> is supercritical above its critical temperature ( $T_c = 33.14$  K), and its density at 100 bar (34.63 mol/L) nearly matches (~98%) the density of LH<sub>2</sub> at atmospheric pressure (35.17 mol/L) [6]. This indicates that, at this limit, the cost of the cooling operation could be reduced without significant losses in storage capacity. In this study, we explore the potential of using MOFs for hydrogen storage where  $T > T_c = 33.14$  K and 100 bar.

We combined molecular simulations and machine learning models to calculate H<sub>2</sub> adsorption uptakes at 34 K (above the critical temperature of H<sub>2</sub>) and 100 bar. The goal was to screen the CoRE MOF database (2019) [7,8] to identify structures that maximize the transport temperature (reducing costs) while maintaining a volumetric energy density close to that of liquid hydrogen.

### 2. Models and methods

#### 2.1. H<sub>2</sub> model

Hydrogen molecules were represented as proposed by Sun et al. [9]. In this model, H<sub>2</sub> molecules are represented by a rigid linear three-site

H-M-H model with an H-M distance of 0.3705 Å, where M corresponds to the center-of-mass (COM) of the molecule. We chose this model because it accurately represents the hydrogen density at 34 K and 100 bar (34.32 mol/L compared to 34.63 mol/L from the NIST database). Table 1 presents the forcefield parameters and atomic charges for hydrogen.

Table 1. Forcefield parameters and atomic charges taken from Sun et al. [9] for H<sub>2</sub> molecules.

Atom	$\sigma$ (Å)	$\epsilon/k_B$ (K)	$q$ (e <sup>-</sup> )
H	3.03	8.03	0.47
M (COM)	-	-	-0.94

## 2.2. Metal-organic framework models

The structures of the metal-organic frameworks were extracted from CoRE database (2019) [7,8]. Forcefield parameters for MOFs atoms were taken from UFF [10]. MOF frameworks were treated as rigid and the atomic charges were neglected.

## 2.3. Simulation details

Adsorption uptakes were calculated using Monte Carlo method in the grand canonical ensemble (GCMC). All calculations were performed with the RASPA 2.0 code [11]. A truncated Lennard-Jones potential with tail correction was used. Periodic boundary conditions and a cutoff radius of 12.8 Å were applied. For the minimum image convention to be satisfied, all unit cells were replicated to at least 25.6 Å along each axis. Lorentz-Berthelot mixing rules were employed to calculate solid-fluid terms. 5 x 10<sup>4</sup> Monte Carlo cycles were employed.

## 2.4. Descriptors

For descriptive variables, we used the following structural characteristics of MOFs: Largest Cavity Diameter (LCD, Å), Pore Limiting Diameter (PLD, Å), Specific Volume (SV, cm<sup>3</sup>/g), Largest Sphere along the Free Path (LSFP, Å), Accessible Surface Area (ASA in m<sup>2</sup>/cm<sup>3</sup>), and Helium Void Fraction (HFV, dimensionless).

## 2.5. Machine Learning Algorithms

As this work fits into a regression problem, the same metrics were used to evaluate the performance of the models: the R<sup>2</sup> coefficient, which can be interpreted as the percentage of variance in the target variable that the independent variables collectively explain, and average absolute relative deviation (AARD%), which returns a sense of how far the predicted data are from the simulated ones.

All models and other data modifications were made with Python through the Jupyter environment, using the Scikit-Learn and TensorFlow packages, libraries specialized in methods for machine learning and model optimization.

**Polynomial Regression:** It is a type of regression that relates dependent and independent variables through a polynomial of the nth degree, which serves as the adjustment parameter for the method.

**Extreme Gradient Boosting:** It works similarly to Random Forest, as it is also based on decision trees. However, this method tests a set of samples sequentially, making it more robust.

**Artificial Neural Network:** Model that is built through layers, being the initial layer constituted by the descriptors; the intermediate layers are made up of a certain number of processing units (neuron), followed by an activation function (for general regression proposals, ReLU is the most indicated [12]), for performing nonlinear transformations, and finally, an output layer consisting of only one neuron, which will make the prediction.

The models' hyperparameters are adjusted during training, using the Grid Search technique. In this next step, to avoid biases of a specific distribution of the data during the separation between training and testing, we use the technique of Cross Validation, dividing in the standard mode of 20% for testing, so that the model obtains an overview of the dataset during the training, rather than just a fixed fraction.

## 3. Results

### 3.1. Forcefield validation

To validate our approach, we calculated the adsorption uptake of H<sub>2</sub> at 77 K in six representative MOFs: IRMOF-1, IRMOF-6, MOF-177, Cu-BTC, MIL-101 (Cr), and ZIF-8. We compared the results with experimental data from the literature [1] (Table 2), which showed satisfactory agreement. It is important to note that the simulated values tend to

overestimate the experimental ones. This discrepancy occurs because the crystal structures used in simulation are idealized, unlike real materials. These results indicate that the applied models and forcefield parameters are suitable for studying hydrogen adsorption in MOFs.

Table 2. Simulated and experimental uptakes of H<sub>2</sub> at 77 K.

MOF	P (bar)	Sim. (% wt)	Exp. (% wt)
IRMOF-1	50	6.2	4.7
IRMOF-6	50	5.8	4.8
MOF-177	70	8.9	7.5
Cu-BTC	50	4.1	3.6
MIL-101	60	6.6	6.1
ZIF-8	55	3.5	3.0

### 3.2. H<sub>2</sub> uptakes for 100 MOFs

H<sub>2</sub> adsorption uptakes at 34 K and 100 bar were calculated for 100 MOFs using GCMC simulations. These structures were randomly selected from the CoRE database. Five of the 100 structures exhibited a volumetric capacity greater than 90% of the density of liquid hydrogen (Table 3). Additionally, we identified that structures with low density and high void fractions demonstrated the best performance, suggesting that these characteristics are key factor in optimizing hydrogen storage at low temperatures.

Table 3. The top five out of the 100 MOF structures.

MOF ID	Density (cm <sup>3</sup> /g)	HVF	Uptake (mol/L)	% LH <sub>2</sub>
NIBHUC	0.449	0.869	34.397	97.8
MUDTEL	0.559	0.85	33.682	95.7
REXGAE	0.654	0.893	32.900	93.5
EPONAA	0.495	0.785	32.579	92.6
NUBPIL	0.608	0.813	32.092	91.2

### 3.3. Machine Learning

The simulated uptakes were used to develop the machine learning models. Normalization was performed to keep the descriptors on the same scale, avoiding a bias that those on the largest scale are artificially determined by larger coefficients in the model function and that they are more erroneously

penalized by regularization techniques, which punish excessively large coefficients.

The performance results of each of the three models are shown in Figures 1. The prediction quality of the models can be verified the smaller the dispersion of the points around the bisector line.

The summary of the metric results for the test set are shown in Table 4, which are used to discriminate the models.

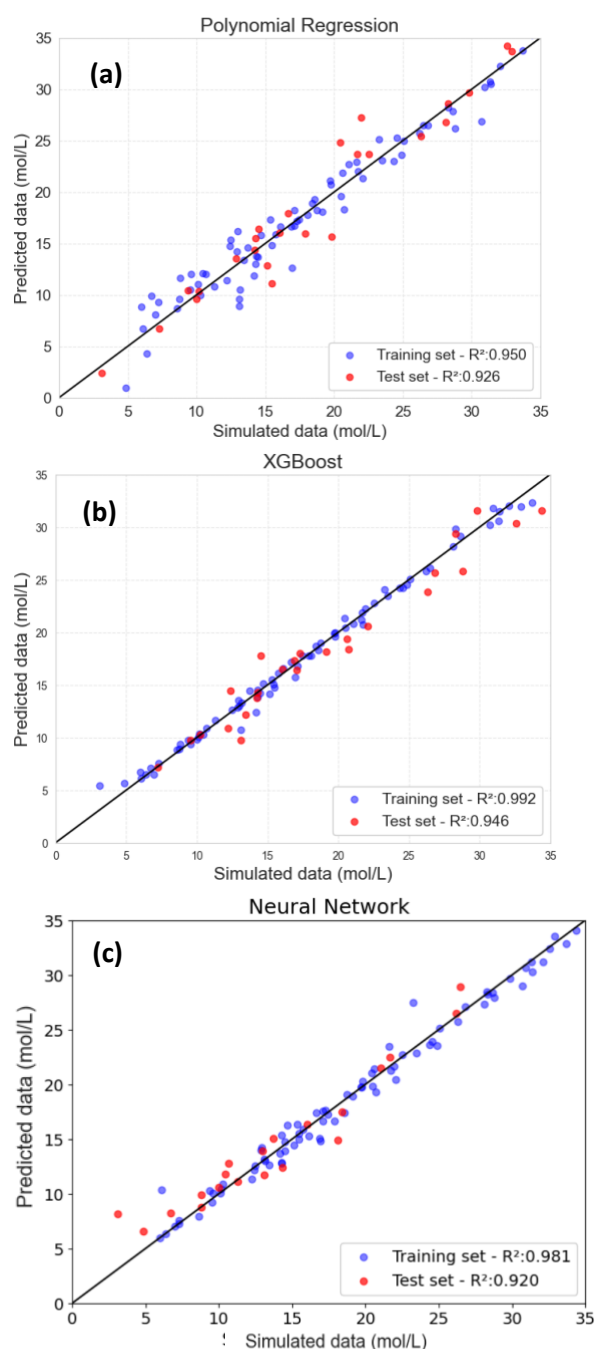


Fig. 1. Prediction results for the models.

Table 4. Discrimination of models for the test set.

ML model	R <sup>2</sup>	AARD%
Polynomial Regression	0.928	17.72
XGBoost	0.947	12.22
Neural Network	0.920	17.50

The XGBoost model presented the best result among the three analyzed, although the polynomial regression (simplest model) proved to be satisfactory for predicting the adsorbed amount of H<sub>2</sub> at 100 bar and 34 K.

The performance of the ANN model was not as satisfactory as expected and a possible explanation is that the network architecture was not optimized enough, as unlike tree-based models, training an ANN is much more costly in time and processing and/or the dataset is small for training the number of weights of the tested architectures.

#### 4. Conclusion

Molecular simulation and machine learning methods were employed to investigate H<sub>2</sub> cryo-adsorption in MOFs. The molecular models and forcefields were validated against experimental data. H<sub>2</sub> adsorption uptakes at 34 K and 100 bar were calculated for 100 structures. These data, along with the structural characteristics of MOFs, were used to develop machine learning models. Among the models evaluated, XGBoost demonstrated the best performance, with an average absolute relative deviation of 12.22%. This model allows for evaluating the performance of MOFs for H<sub>2</sub> storage and transportation under cryogenic conditions, significantly reducing the time and costs associated with identifying optimal structures.

#### Acknowledgements

The authors would like to thank FUNCAP, CAPES, and CNPq for the financial support and the use of computer cluster at National Laboratory of Scientific Computing (LNCC/MCTI, Brazil).

#### References

- [1] T.K.P. Myunghyun Paik Suh, Hye Jeong Park, *Chem. Rev.* 112(112) (2012) 782–835.
- [2] J. Park., J. Ha., R. Muhammad., H.K. Lee., R. Balderas-Xicohtencatl., Y. Cheng., A.J. Ramirez-Cuesta., B. Streppel., M. Hirscher., H.R. Moon., H. Oh, *ACS Appl. Energy Mater.* 6(18) (2023) 9057–64. 10.1021/acsaem.2c01907.
- [3] H. Oh., D. Lupu., G. Blanita., M. Hirscher, *RSC Adv.* 4(6) (2014) 2648–51. 10.1039/c3ra46233a.
- [4] M. Gardiner, *U.S Dep. Energy* 25 (2009) 1–6.
- [5] M.D. Allendorf., Z. Hulvey., T. Gennett., A. Ahmed., T. Autrey., J. Camp., E. Seon Cho., H. Furukawa., M. Haranczyk., M. Head-Gordon., S. Jeong., A. Karkamkar., D.J. Liu., J.R. Long., K.R. Meihaus., I.H. Nayyar., R. Nazarov., D.J. Siegel., V. Stavila., J.J. Urban., S.P. Veccham., B.C. Wood, *Energy Environ. Sci.* 11(10) (2018) 2784–812. 10.1039/c8ee01085d.
- [6] NIST, *NIST Stand. Ref. Database* 173 (2017). 10.18434/T4M88Q.
- [7] Y.G. Chung., J. Camp., M. Haranczyk., B.J. Sikora., W. Bury., V. Krungleviciute., T. Yildirim., O.K. Farha., D.S. Sholl., R.Q. Snurr, *Chem. Mater.* 26(21) (2014) 6185–92. 10.1021/cm502594j.
- [8] Y.G. Chung., E. Haldoupis., B.J. Bucior., M. Haranczyk., S. Lee., H. Zhang., K.D. Vogiatzis., M. Milisavljevic., S. Ling., J.S. Camp., B. Slater., J.I. Siepmann., D.S. Sholl., R.Q. Snurr, *J. Chem. Eng. Data* 64(12) (2019) 5985–98. 10.1021/acs.jced.9b00835.
- [9] Y. Sun., R.F. DeJaco., Z. Li., D. Tang., S. Glante., D.S. Sholl., C.M. Colina., R.Q. Snurr., M. Thommes., M. Hartmann., J. Ilja Siepmann, *Sci. Adv.* 7(30) (2021). 10.1126/sciadv.abg3983.
- [10] A.K. Rappé., C.J. Casewit., K.S. Colwell., W.A. Goddard III., W.M. Skid, *J. Am. Chem. Soc.* 114 (1992) 10024–35. 10.1021/ja00051a040.
- [11] D. Dubbeldam., S. Calero., D.E. Ellis., R.Q. Snurr, *Mol. Simul.* 42(2) (2016) 81–101. 10.1080/08927022.2015.1010082.
- [12] C. Bircanoğlu., N. Arica, *26th Signal Processing and Communications Applications Conference*, 2018, pp. 1–4.